ICRU REPORT 55

Secondary Electron Spectra from Charged Particle Interactions

Issued: 20 April 1996

INTERNATIONAL COMMISSION ON RADIATION
UNITS AND MEASUREMENTS
7910 WOODMONT AVENUE
BETHESDA, MARYLAND 20814
U.S.A.

THE INTERNATIONAL COMMISSION ON RADIATION UNITS AND MEASUREMENTS

INDIVIDUALS PARTICIPATING IN THE PREPARATION OF THIS REPORT

Commission Membership during Preparation of this Report

A. ALLISY, *Chairman*
A. M. KELLERER, *Vice Chairman*
R. S. CASWELL, *Secretary*
G. E. D. ADAMS
K. DOI
L. FEINENDEGEN
M. INOKUTI
I. ISHERWOOD
J. R. MALLARD
H. PARETZKE
H. H. ROSSI
A. WAMBERSIE
G. F. WHITMORE
L. S. TAYLOR, *Honorary Chairman and Member Emeritus*

Current Commission Membership

A. ALLISY, *Chairman*
A. WAMBERSIE, *Vice Chairman*
R. S. CASWELL, *Secretary*
P. M. DELUCA, JR.
K. DOI
L. FEINENDEGEN
M. INOKUTI
I. ISHERWOOD
H. MENZEL
H. PARETZKE
H. H. ROSSI
G. F. WHITMORE
L. S. TAYLOR, *Honorary Chairman and Member Emeritus*

Commission Sponsors

M. INOKUTI
Argonne National Laboratory
Argonne, Illinois, U.S.A.

H. PARETZKE
Gesellschaft für Strahlen- und Umweltforschung
Neuherberg bei München, Germany

Report Committee

M. E. RUDD, *Chairman*
University of Nebraska
Lincoln, Nebraska, U.S.A.

Y.-K. KIM
National Institute of Standards and Technology
Gaithersburg, Maryland, U.S.A.

T. MÄRK
Universität Innsbruck
Innsbruck, Austria

J. SCHOU
Risø National Laboratory
Roskilde, Denmark

N. STOLTERFOHT
Hahn-Meitner-Institut Berlin
Berlin, Germany

L. H. TOBUREN
National Academy of Sciences
Washington, DC, U.S.A.

Consultants to the Report Committee

H. BICHSEL
Seattle, Washington, U.S.A.

R. D. DUBOIS
Pacific Northwest Laboratory
Richland, Washington, U.S.A.

Principal Scientific Counsellor

H. O. WYCKOFF

Assistant Secretary

W. R. NEY

Managing Editor of ICRU NEWS

H. G. EBERT

Counselor to the Commission on Financial Affairs

O. LINTON

The Commission wishes to express its appreciation to the individuals involved in the preparation of this Report f the time and effort which they devoted to this task and to express its appreciation to the organizations with which th are affiliated.

(For detailed information of the availability of this and other ICRU Reports, see page 109.)

Preface

Scope of ICRU Activities

The International Commission on Radiation Units and Measurements (ICRU), since its inception in 1925, has had as its principal objective the development of internationally acceptable recommendations regarding:

1. Quantities and units of radiation and radioactivity,
2. Procedures suitable for the measurement and application of these quantities in clinical radiology and radiobiology and
3. Physical data needed in the application of these procedures, the use of which tends to assure uniformity in reporting.

The Commission also considers and makes similar types of recommendations for the radiation protection field. In this connection, its work is carried out in close cooperation with the International Commission on Radiological Protection (ICRP).

Policy

The ICRU endeavors to collect and evaluate the latest data and information pertinent to the problems of radiation measurement and dosimetry and to recommend the most acceptable values and techniques for current use.

The Commission's recommendations are kept under continual review in order to keep abreast of the rapidly expanding uses of radiation.

The ICRU feels that it is the responsibility of national organizations to introduce their own detailed technical procedures for the development and maintenance of standards. However, it urges that all countries adhere as closely as possible to the internationally recommended basic concepts of radiation quantities and units.

The Commission feels that its responsibility lies in developing a system of quantities and units having the widest possible range of applicability. Situations may arise from time to time when an expedient solution of a current problem may seem advisable. Generally speaking, however, the Commission feels that action based on expediency is inadvisable from a long-term viewpoint; it endeavors to base its decision on the long-range advantages to be expected.

The ICRU invites and welcomes constructive comments and suggestions regarding its recommendations and reports. These may be transmitted to the chairman.

Current Program

The Commission has divided its field of interest into 12 technical areas and has assigned one or more members of the Commission the responsibility for identification of potential topics for new ICRU activities in each area. Each area is reviewed periodically by its sponsors. Recommendations for new reports are then reviewed by the Commission and a priority assigned. The technical areas are:

Radiation Therapy
Diagnostic Radiology
Nuclear Medicine
Radiobiology
Radioactivity
Radiation Physics— X Rays, Gamma Rays and Electrons
Radiation Physics— Neutrons and Heavy Particles
Radiation Protection
Radiation Chemistry
Critical Data
Theoretical Aspects
Quantities and Units

The actual preparation of ICRU reports is carried out by ICRU report committees. One or more Commission members serve as sponsors to each committee and provide close liaison with the Commission. The currently active report committees are:

Absorbed Dose Standards for Photon Irradiation and Their Dissemination
Beta-Ray Dosimetry for Radiation Protection
Clinical Dosimetry for Neutrons (Specification of Beam Quality)
Determination of Body Burdens for Radionuclides
Dose Specification for Reporting Interstitial Therapy
Dosimetric Procedures in Diagnostic Radiology
Fundamental Quantities and Units
Mammography — Assessment of Image Quality
Medical Application of Beta Rays
Nuclear Data
Prescribing, Recording and Reporting Electron Beam Therapy
Proton Therapy
ROC Analysis
Radiobiology Specification of Beam Quality and Specification of Therapy Parameters
Relationship between Quantities for Radiological Protection against External Radiation (Joint ICRP-ICRU Task Group)
Requirements for Radioecological Sampling
Statistical Aspects of Environmental Sampling
Stopping Power for Heavy Ions
Tissue Substitutes, Characteristics of Biological Tissue and Phantoms for Ultrasound

ICRU's Relationships with Other Organizations

In addition to its close relationship with the ICRP, the ICRU has developed relationships with other organizations interested in the problems of radiation quantities, units and measurements. Since 1955, the ICRU has had an official relationship with the World Health Organization (WHO), whereby the ICRU is looked to for primary guidance in matters of radiation units and measurements and, in turn, the WHO

assists in the world-wide dissemination of the Commission's recommendations. In 1960, the ICRU entered into consultative status with the International Atomic Energy Agency. The Commission has a formal relationship with the United Nations Scientific Committee on the Effects of Atomic Radiation (UNSCEAR), whereby ICRU observers are invited to attend UNSCEAR meetings. The Commission and the International Organization for Standardization (ISO) informally exchange notifications of meetings, and the ICRU is formally designated for liaison with two of the ISO technical committees. The ICRU also corresponds and exchanges final reports with the following organizations:

Bureau International de Métrologie Légale
Bureau International des Poids et Mesures
Commission of the European Communities
Council for International Organizations of Medical Sciences
Food and Agriculture Organization of the United Nations
International Council of Scientific Unions
International Electrotechnical Commission
International Labor Office
International Organization for Medical Physics
International Radiation Protection Association
International Union of Pure and Applied Physics
United Nations Educational, Scientific and Cultural Organization

The Commission has found its relationship with all of these organizations fruitful and of substantial benefit to the ICRU program. Relations with these other international bodies do not affect the basic affiliation of the ICRU with the International Society of Radiology.

Operating Funds

In the early days of its existence, the ICRU operated essentially on a voluntary basis, with the travel and operating costs being borne by the parent organization of the participants. (Only token assistance was originally available from the International Society of Radiology.) Recognizing the impractibility of continuing this mode of operation on an indefinite basis, operating funds were sought from various sources.

During the last 10 years, financial support has been received from the following organizations:

American Society for Therapeutic Radiology and Oncology
Atomic Energy Control Board
Bayer AG
Central Electricity Generating Board
Commissariat à l'Énergie Atomique
Commission of the European Communities
Dutch Society for Radiodiagnostics
Eastman Kodak Company
Ebara Corporation
Électricité de France
Fuji Medical Systems
General Electric Company
Hitachi, Ltd.
International Atomic Energy Agency
International Radiation Protection Association
International Society of Radiology
Italian Radiological Association
Japan Industries Association of Radiation Apparatus
Konica Corporation
National Cancer Institute of the U.S. Department of Health and Human Services
National Electrical Manufacturers Association
Philips Medical Systems, Incorporated
Radiation Research Society
Scanditronix AB
Siemens Aktiengesellschaft
Sumitomo Heavy Industries, Ltd.
Theratronics
Toshiba Corporation
University Hospital Lund, Sweden
World Health Organization

In addition to the direct monetary support provided by these organizations, many organizations provide indirect support for the Commission's program. This support is provided in many forms, including, among others, subsidies for (1) the time of individuals participating in ICRU activities, (2) travel costs involved in ICRU meetings and (3) meeting facilities and services.

In recognition of the fact that its work is made possible by the generous support provided by all of the organizations supporting its program, the Commission expresses its deep appreciation.

André Allisy
Chairman, ICRU

Sévres, France
20 March 1996

Abstract

This report provides a comprehensive guide to quantitative information about emission of secondary electrons in collisions of fast electrons, protons, alpha particles, and heavier ions with free atoms and molecules and with condensed matter. Explanations of the various mechanisms of ionization are given. Experimental methods are described, and theoretical techniques are presented for determining total cross sections as well as cross sections differential in the ejection angle and energy of the secondary electrons. The semi-empirical and analytical models given enable the user to make rapid calculations of certain cross sections. Some applications of secondary electron spectra to radiological problems are also described. Data are available for impacts by electrons at energies from a few eV up to 10 keV, for incident protons from a few keV up to 5 MeV, and for heavier particles up to 1000 MeV. Methods are described for extrapolating cross section data to higher energies. The wide variety of targets reviewed include atoms (H, He, Ne, Ar, Kr, Xe, and Hg), molecules (H_2, N_2, O_2, CO_2, H_2O, CH_4, C_2H_2, C_3H_8, C_6H_6, and CH_3NH_2), and solids (C, Al, Pb, and Au). Some of the calculational methods can be used for all targets for which basic data, such as ionization potentials, are available.

Contents

Glossary

Fundamental constants

e	charge of the electron $\simeq 1.60 \times 10^{-19}$ C
a_0	Bohr radius $\simeq 5.29 \times 10^{-11}$ m
v_0	Bohr orbital speed $\simeq 2.19 \times 10^{6}$ m/s
m_e	mass of an electron $\simeq 9.11 \times 10^{-31}$ kg
λ	ratio of projectile to electron mass (*e.g.*, $\lambda = 1$ for electrons, $\lambda \simeq 1836$ for protons)
R	Rydberg energy $\simeq 13.6$ eV

Pre-collision quantities

E	kinetic energy of the incident particle (projectile)
$T = E/\lambda$	kinetic energy of an electron with same velocity as the incident particle (for electron impact, $T = E$)
$t = T/B$	reduced incident energy
Z_1	nuclear charge (atomic number) of the incident particle
Z_2	nuclear charge (atomic number) of the target particle
q	net charge of the incident particle (for bare incident particles, $q = Z_1$)
B, (B_i)	binding energy of a target electron (in the ith subshell)
U, (U_i)	average kinetic energy of a target electron (in the ith subshell)
N, (N_i)	occupation number or number of electrons (in the ith subshell)
n	number of target particles per unit volume

Post-collision quantities

Q	energy transfer in the collision
ϵ	energy of a secondary electron
$w = \epsilon/B$	reduced secondary electron energy
θ	angle between the direction of the secondary electron and initial direction of the incident particle
$\bar{\epsilon}$	average secondary electron energy
W	average energy required to make an electron-ion pair

Cross sections

$\sigma(\epsilon, \theta)$	doubly differential cross section for ejection of a secondary electron of energy ϵ at angle θ
$\sigma(\epsilon)$	singly differential cross section for ejection of a secondary electron of energy ϵ
$\sigma(\theta)$	singly differential cross section for ejection of a secondary electron at angle θ
σ_i	total (or integral) cross section for ejection of secondary electrons

Other

df/dQ	differential continuum oscillator strength
M_i^2	dipole matrix element squared, and measured in a_0^2
$\mathscr{E}$	electric field
δ	total yield of electrons from a surface
η	yield of electrons reflected from a surface
ϵ^L	dielectric constant

Abbreviations

BE	binary encounter
BEA	binary encounter approximation
BEA-F	binary encounter approximation with Fock distribution
BEAX	binary encounter approximation with exchange
BEB	binary encounter-Bethe
BED	binary encounter-dipole
CDW-EIS	continuum-distorted-wave/Eikonal-initial state
CTMC	classical trajectory Monte Carlo

DDCS	doubly differential cross section
DDCS-MT	doubly differential cross section-mixed treatment
DM	Deutsch and Märk
DWBA	distorted wave Born approximation
ECC	electron capture to the continuum
GOS	generalized oscillator strength
LET	linear energy transfer
PWBA	plane wave Born approximation
RBE	relative biological effectiveness
SCEE	single-center electron emission
SDCS	singly differential cross section
TCEE	two-center electron emission
TICS	total ionization cross section, σ_i
UHV	ultrahigh vacuum

Note: The definitions of the quantities e, E, Q, and σ (for cross section) are consistent with those in ICRU Report 16 (ICRU, 1970)

Secondary Electron Spectra from Charged Particle Interactions

1. Introduction

1.1 Purpose and Scope

Fast charged particles traversing matter lose energy through successive collisions with the atoms and molecules of the material. The simplest index characterizing the energy loss of an incident charged particle is the stopping power, which is the mean energy loss per unit path length in a material.

Because the stopping power is fundamental to dosimetry, instrumentation design, modeling of radiation effects, and other uses, the ICRU has conducted a long-term survey of stopping powers of materials of radiological and dosimetric relevance in order to establish and disseminate standard data sets. This effort has resulted in Report 37, Stopping Powers for Electrons and Positrons (ICRU 1984) and Report 49, Stopping Powers and Ranges for Protons and Alpha Particles (ICRU 1993).

A full consideration of radiation absorption, however, requires more detailed information than is provided by the stopping power. Because most of the contribution to the collision stopping power for fast charged particles is due to the production of ions and secondary electrons, a knowledge of the probabilities for ionization is needed. And because some of the secondary electrons, known in radiological work as *delta rays*, are energetic enough to travel a considerable distance and to cause further excitation and ionization, knowledge of the distribution of their energies and directions is also necessary. The probabilities for specified processes, such as secondary electron production, are described in atomic physics by the concept of *cross section*, which will be discussed in the next section.

The study of secondary electron emission in atomic collisions began in the 1930s, but measurements of a large range of atomic collision cross sections were not made until the 1960s. Energy and angular distributions of secondary electrons were also studied at that time, both experimentally and theoretically, and several mechanisms for ionization were identified, some of which are still being investigated. Compilations and critical reviews of data, though still few in number, have begun to appear, and a number of empirical or semiempirical analytical models have been devised to describe cross sections. Our understanding of collisional ionization is not yet complete, but since the important mechanisms have been identified and their systematics generally understood, it is timely to gather such information into a report accessible to potential users of such data.

This report deals primarily with interactions of charged particles although some attention is given to ionization by neutral particle impact. The emphasis is on the energy spectra of secondary electrons produced in ionizing collisions because of their importance in radiological work, but angular distributions of ejected electrons are also considered because they determine the spatial characteristics of the energy deposition. Most of the studies to date have used rarified gas targets in order to focus on the characteristics of energy loss in single collisions with isolated atoms or molecules. For such targets, experimental data for electron collisions are now available for impact energies of a few electron volts (eV) up to several thousand electron volts (keV), for proton impact from a few keV to several million electron volts (MeV) and for heavier particles from a few keV up to about a thousand MeV. Because of experimental difficulties and the complexities of theoretical descriptions, studies of secondary electron production in condensed matter are not as numerous and our understanding is not as far advanced.

After a presentation of the concepts involved and a brief introduction to the relationship of secondary electron data to radiological questions, the report addresses in Section 2 the theoretical methods by which ionization processes can be described and understood. A description of several treatments is given along with a set of consistency requirements, based on theory, by which the reliability of experimental data can be judged. Sections 3 and 4 consider electron and ion interactions and describe the experimental methods, the interaction mechanisms, data, and specific theoretical methods and analytical models pertaining to each type of interaction. Secondary electron production in condensed matter is reviewed in Section 5. Section 6 describes some applications of the data on electron spectra to radiobiology that may be made using the present state of our knowledge of ionization.

1.2 Notation and Concepts

When an energetic charged particle undergoes a collision with an atom or molecule, a number of basic processes can take place, the most important of which are:

Ionization: This is the ejection of one or more electrons in the collision. Kinetic energy from the primary particle is used to overcome the binding energy and to give kinetic energy to the secondary electron(s).

Electron transfer: In the case of ion impact, one or more electrons can be transferred from the target to the incident ion or vice versa. The loss of kinetic energy of the projectile is equal to the difference in binding energies of the electron in the initial and final states. In rare cases, this results in an increase in the kinetic energy of the projectile.

Excitation: One or more electrons in the target or the projectile are put into higher energy (excited) bound states, the increase in energy coming from the kinetic energy of the projectile. This is sometimes followed by the emission of a photon.

Dissociation: In the case of diatomic, or larger, molecules, the transfer of energy in the collision may result in excitation of the molecule which then relaxes with the concurrent separation of the molecule into fragments or with emission of photons. The loss of energy by the projectile is equal to the dissociation energy plus the kinetic as well as internal energy of the fragments. Combinations of these basic processes are also possible and may even be more likely to occur than the simple processes. This report deals only with ionization.

Because of the importance of the concept of electron ejection cross section in our discussion, we next define it in its different forms. Consider a monoenergetic beam of charged particles traversing a medium of sufficiently low density that there is a negligibly small probability that any one of the particles of the beam will make more than one collision. Then the number of electrons N_s ejected along the beam path is proportional to N_0, the number of beam particles passing; to n, the number of target particles per unit volume; and to L, the length of beam path from which the ejected electrons are collected. Thus,

$$N_s = N_0 n L \sigma_i, \tag{1.1}$$

where σ_i is the constant of proportionality. Since this constant must have dimensions of area to be dimensionally consistent, it is called a *cross section*, in this case the total ionization cross section (TICS). Because of the possibility of ejection of more than one electron in a single collision, a distinction is made between the "counting" ionization cross section, σ_c, which refers to the number of ionizing collisions, and the ionization cross section, σ_i, which refers to the total number of electrons emitted. If N_{mz} is the number of slow ions with mass-to-charge ratio m/z resulting from the collision, then the corresponding *partial ionization cross section*, σ_{mzi}, is defined by

$$N_{mz} = N_0 n L \sigma_{mzi}. \tag{1.2}$$

In cases where electron transfer and dissociation are negligible or not present at all, we have the relations

$$\sigma_i = \Sigma\, z\sigma_{mzi} \quad \text{and} \quad \sigma_c = \Sigma\, \sigma_{mzi}. \tag{1.3}$$

In this report σ_i is usually the cross section of most interest.

Information about the energy spectrum of secondary electrons as well as their angular distribution is contained in the doubly differential cross section (DDCS) $d^2\sigma/d\epsilon d\Omega$, where ϵ is the secondary electron energy and Ω is the solid angle into which the electron is ejected. This cross section, which has dimensions of area per unit energy per unit solid angle, is also denoted by $\sigma(\epsilon, \theta)$ since, in practical situations, it is independent of the azimuthal angle ϕ and depends only on the polar angle θ measured relative to the direction of the incident beam. It is defined such that the product $N_0 n L\, \Delta\Omega \Delta\epsilon\, \sigma(\epsilon, \theta)$ represents the number of electrons ejected from a length L of the beam in the target into an element of solid angle $\Delta\Omega$ at a polar angle θ within the energy range ϵ to $\epsilon + \Delta\epsilon$.

For some purposes, the direction of emission of the electron is unimportant and only the spectrum of energies is relevant. This information is contained in the singly differential cross section (SDCS) denoted by $\sigma(\epsilon)$. This quantity, which has dimensions of area per unit energy, is obtained from the DDCS by integrating over all directions of emission:

$$\sigma(\epsilon) = \int \sigma(\epsilon, \theta) d\Omega = 2\pi \int_0^{\pi} \sigma(\epsilon, \theta) \sin\theta\, d\theta. \tag{1.4}$$

The TICS σ_i is the integral of the SDCS,

$$\sigma_i = \int_0^{\epsilon_{max}} \sigma(\epsilon)\, d\epsilon, \tag{1.5}$$

where ϵ_{max} is the maximum energy of ejected electrons.

It is possible to define an even more detailed cross section by also specifying the directions and energies of the projectile after the collision. These multidimensional quantities, traditionally called triply differential cross sections, will not be discussed in this report since few measurements of that type have been made and they have found little application in radiological applications.

1.3 The Role of Secondary Electron Data in Radiological Sciences

The principal method of energy dissipation by ionizing radiation is, by definition, the separation of electrons from the atoms and molecules of the medium in which it is absorbed (Lea, 1947). Therefore, to understand the fundamental processes leading to

production of radiation-induced damage, one must have an understanding of the systematics of electron liberation in ionization and their interaction with matter. Ionization and the resulting electrons initiate most of the molecular changes that are ultimately responsible for the observed biological effects. However, information on excitation may be needed as well.

To describe the initial spatial pattern of products of energy deposition by charged particles one often turns to models for energy deposition and transport (Paretzke, 1987). For the most comprehensive of these models, one must have a knowledge of the absolute cross sections for electron production and their subsequent interactions with the medium of interest. Cross sections are required for such processes as:

- Ionization: DDCSs provide information on spatial patterns of energy deposition, SDCSs are needed to obtain information on the energy loss per ionization event, and TICSs yield information on the mean free path between ionizing events.
- Excitation: Cross sections are needed for production of all excited states of the medium by all charged particles at all relevant energies.
- Electron transfer: Cross sections are needed for capture of electrons into all of the states of the projectile and, in principle, from all initial bound states of the electrons.
- Multiple ionization: Cross sections are needed for the production of residual ions in various charge states to aid in understanding subsequent chemical reactions. Cross sections are also needed for the number and the energies and angles of emission of each of the electrons ejected in a single collision to provide information on the spatial and temporal correlation of ionization events.
- Simultaneous projectile and target ionization: Cross sections are needed for simultaneous ionization of the target and projectile in collisions involving incident particles carrying bound electrons to provide information on the spatial and temporal correlation of ionization events.
- Molecular dissociation: Cross sections or branching ratios are needed for the production of all molecular fragments following ionization and excitation.

1.4 Guide for Users

This section provides a guide for quick access to sections of this report where specific types of cross section data can be found. Such data can be obtained in three basic ways. First, theoretical models. These can be used to obtain data at any given values of parameters with only fundamental constants as input. However, they may require lengthy computations and have resricted ranges of validity. Second, semi-empirical or analytical models. These are simple to apply, but usually require knowledge of adjustable fitting parameters. The present report gives, for example, fitting parameters for one model that can be used to generate reasonably accurate differential cross sections for proton impact on ten different targets for all proton and secondary electron energies. Third, experimental data. Tables of such data may be used directly, but are cumbersome and often require extrapolation or interpolation. Experimental data are most useful when a critical reviewer has chosen recommended or best values from among the available measurements. This choice may be presented as parameters in an analytical model. Measured cross sections are typically reliable to about 15% with a greater uncertainty for slow incident particles and low-energy secondary electrons.

The subsections where the relevant information can be found are identified in the following list.

Electrons incident on gases

Total ionization cross sections

Born approximation: 2.6, 2.7
Bethe approximation: 2.8
Gryzinski equation: 3.3.2
Binary Encounter Approximation (BEA): 2.5, 3.3.2
Classical Trajectory-Monte Carlo (CTMC) method: 2.12
Deutsch-Märk (DM) method: 3.3.2
Khare method: 3.3.2
Binary-Encounter-Dipole (BED) and Binary-Encounter-Bethe (BEB) methods: 3.3.2, 3.6.2.1, and 3.6.2.2
Recommended experimental cross sections for He, Ne, H_2, N_2, O_2, H_2O, CO_2, CH_4, and C_3H_8: 3.3.4

Partial ionization cross sections

Recommended experimental cross sections for Ne, Ar, H_2, N_2, O_2, H_2O, CO_2, and C_3H_8: 3.4.4

Differential cross sections

Rutherford equation: 2.3
Mott equation: 2.4
Binary Encounter Approximation (BEA): 2.5
Born Approximation 2.6, 2.7
Bethe approximation 2.8
Classical Trajectory-Monte Carlo (CTMC) method: 2.2, 2.12
Khare method 3.6.2
Binary-Encounter-Dipole (BED) and Binary-Encounter-Bethe (BEB) methods: 3.6.2.1 and 3.6.2.2
Rudd equation: 3.6.2
Compilation of experimental reports for H, He, Ne, Ar, Kr, Xe, Hg, H_2, N_2, O_2, CH_4, NH_3, H_2O, $(H_2O)_n$, C_2H_2, CO, NO, and CO_2: Table 3.4 in 3.6.3
Recommended experimental cross sections: 3.6.3

Protons incident on gases

Total ionization cross sections

Born approximation: 2.6, 2.7
Bethe approximation: 2.8
Binary Encounter Approximation (BEA): 2.5, 4.4.1
Classical Trajectory-Monte Carlo (CTMC) method: 2.12
Doubly Differential Cross Section-Mixed Treatment (DDCS-MT): 4.4.2
Recommended experimental cross sections for H, He, Ne, Ar, Kr, Xe, H_2, N_2, O_2, CO, CO_2, NH_3, CH_4, and H_2O: 4.6.1

Differential cross sections

Born approximation: 2.6, 4.4.2
Continuum Distorted Wave-Eikonal Initial State (CDW-EIS) method: 2.11
Classical Trajectory-Monte Carlo (CTMC) method: 2.12
Miller model: 4.5.1
Rudd model with parameters for He, Ne, Ar, Kr, H_2, N_2, O_2, H_2O, CO_2, and CH_4: 4.5.2
Kim model with parameters for Ar and N_2: 4.5.3
Hansen-Kocbach-Stolterfoht (HKS) model: 4.5.4
List of experimental reports for H, He, Ne, Ar, Kr, Xe, H_2, N_2, O_2, H_2O, CO_2, NH_3, SF_6, TeF_6, CH_4, C_2H_2, C_2H_4, C_2H_6, C_6H_6, CH_3NH_2, $(CH_3)_2NH$: Table 4.5 in 4.6.2
List of reviews of data: 4.6.2
Recommended experimental values: 4.6.2

Other heavy particles incident on gases

Differential cross sections

List of experimental and theoretical reports for He, Ne, Ar, Kr, H_2, H_2O, and CH_4: Tables 4.6-4.8 in 4.7.4

Particles incident on condensed matter

Graphical experimental data for Al: 5.5, 5.8; Au: 5.1, 5.2, 5.7, 5.8; C: 5.3.3, 5.7, 5.8, 5.10; Cu: 5.8; Fe: 5.8; Nb: 5.1; Sn: 5.8
Dielectric response theory: 5.3.1
Gryzinski equation: 5.3.2

2. Theoretical Methods

2.1 Introduction

The methods presented in this section for describing collisional ionization form the basis for many theoretical treatments of energy absorption in irradiated matter. The discussion here is equally applicable to collisions with individual atoms or molecules but needs to be modified for condensed matter. For brevity we shall use the term target "atoms" to include molecules as well, unless specified otherwise.

In addition to information on excitation and other energy-loss processes, ionization cross sections at all projectile and secondary electron energies are needed to follow the history of an incident particle and its products, covering all ranges of energy transferred in individual collisions. What is most relevant to a collision theory is not the incident energy but the speed of the incident particle, whether it is a bare charged particle or a particle with its own internal structure. For a very fast projectile, the interaction between the projectile and the target atom can be treated as a perturbation, while a slow electron or ion forms a transient compound system with the target, a transient negative ion, or a diatomic or polyatomic molecule, depending on the projectile and the target. The formation of a compound system complicates the theoretical description of such a system and is the basic reason that the theoretical formulation of a slow collision is far more difficult than the treatment of a fast collision.

A collision of an electron with a target atom is most accurately described by using quantum mechanical descriptions for both the projectile and the target. Since the projectile electron is indistinguishable from an electron in the target, all electrons in the colliding system must satisfy the Pauli exclusion principle. This principle is satisfied by making the wave function for the total system (projectile plus target) antisymmetric with respect to the interchange of electron labels. The use of antisymmetrized wave functions leads to two kinds of interaction matrix elements—direct and exchange. Direct terms dominate cross sections for ordinary collisions, especially for fast incident electrons, while exchange terms become appreciable in slow collisions. Also, exchange terms dominate cross sections for collisions that change the total spin states of the target. After an ionizing collision, the scattered and ejected electrons cannot be distinguished; customarily the faster electron is called the *primary* electron and the slower one the *secondary* electron. We shall also refer to all electrons ejected by collisions of any heavier projectiles—protons, α-particles, etc.—as secondary electrons.

Collisions involving bare ion projectiles, unless they are very slow, can be treated by using a classical description for the trajectory of the projectile with a quantal description of the target. This approach is known as the semiclassical theory. For incident ions with speeds comparable to or lower than the orbital speeds of the bound electrons in the target, the capture of electrons from the target is a significant mechanism that ionizes the target but does not produce secondary electrons. Also, due to restrictions imposed by the conservation of momentum and energy, an incident heavy particle can impart only a small fraction of its kinetic energy to the target electron (unless the binding energy is an appreciable fraction of the incident energy).

If the projectile is a neutral atom or a dressed ion (*i.e.*, an ion bearing one or more electrons), a collision can eject electrons from either the projectile or the target. For a fast projectile, one can consider the projectile as a simple collection of a nucleus and electrons travelling together at the same speed. Each constituent of the projectile then collides with the target as if it were an independent incident particle. Excitation and ionization of the projectile by the target can be handled by simply reversing the frame of reference, *i.e.*, the target impinges on the projectile with the same relative speed. A slow collision of this type, however, will form a transient molecule and then break up, sometimes with a violent disruption in the shell structure of the target and/or the projectile.

There are two elements in a collision theory: the treatment of the projectile-target interaction and the description of the target atom (and the projectile, too, if it has its own internal structure). The former can be formulated using a classical approach; the latter invariably requires a quantal formulation. As is evident from the preceding discussions, there are different interaction mechanisms peculiar to each kind of projectile in addition to the usual binary collisions between the projectile and a bound electron in the target. In this section, we outline theories that serve as the common foundation for further refinements for different types of projectiles. Specific applications will be discussed in the sections dealing with different types of projectiles.

2.2 Doubly Differential Cross Sections

In the collision of two free charged particles, the recoil energy and angle of the target particle are uniquely related by conservation of energy and momentum, and thus the angular distribution for a given recoil energy is a δ-function. For a bound electron, however, the residual ion gets a share of the total momentum transferred to the target, and an electron of a specified energy may be ejected in any

direction. When the electron takes most of the transferred momentum, the angular distribution is sharply peaked in the direction of the momentum transfer, yielding what is called the binary-encounter (BE) peak. Fast electrons ejected in collisions with small impact parameters are concentrated near the binary-collision peak. For the nonrelativistic case, the direction of the BE peak is given by

$$\cos\theta_B = \frac{M + m_e}{2M}\sqrt{\frac{MQ}{m_e E}}, \qquad (2.1)$$

where θ_B is measured from the direction of the incident beam, m_e is the electron rest mass, M and E are the mass and kinetic energy, respectively, of the incident particle, and the energy transfer Q is defined in terms of the ejected electron energy ϵ and the binding energy B:

$$Q = \epsilon + B. \qquad (2.2)$$

The width of the binary-collision peak is linked to how tightly the target electron is bound; the higher the binding energy, the broader is the binary-collision peak. The shape of the peak is determined by the distribution of momenta of the target electrons prior to the collisions.

While fast secondary electrons result from close (*i.e.*, nearly head-on) collisions, slow electrons come from distant or glancing collisions. For slow electrons the angular distribution is the superposition of the binary encounter peak and the angular distribution characteristic of the dipole interaction. This results in a broad peak centered at $\theta_B \sim 60°$ to 80°. A positive ion projectile, especially a highly charged one, tends to focus the ejected electrons in the forward direction, at the same time depleting electrons ejected in the backward direction.

Many collision theories, such as the Rutherford theory and the first Born approximation (FBA), simply scale cross sections according to Z_1^2, where $Z_1 e$ is the charge of the projectile. For slow projectiles, however, this scaling is invalid because an ejected electron feels attractive forces from both the scattered projectile and the parent ion. This is part of a more general interaction mechanism known as the two-center effect (see Section 4.2.1). Of the several competing theories proposed to account for the two-center effects, the continuum-distorted-wave, eikonal-initial-state (CDW-EIS) method (Fainstein *et al.*, 1991b) has been particularly successful in reproducing many qualitative features of the two-center effects. This method uses continuum wave functions for the ejected electron that refer to the effective nuclear charges of both the residual ion and the incident ion.

Another approach in calculating DDCSs for ionization by heavy ions is the classical-trajectory Monte Carlo (CTMC) method developed by Olson (1983) and co-workers. In this method, various impact conditions for the projectile are chosen randomly and their trajectories are calculated using classical Coulomb interactions between the projectile, the target nucleus and the target electron. The target electron is identified by its orbit around the nucleus, but no explicit wave functions are used to describe the target atom. Further discussion of the CDW-EIS and the CTMC method are given in Sections 2.11 and 2.12. These methods are particularly effective for ionization by heavy ions.

2.3 Rutherford Cross Section

The scattering of two charged, structureless particles was described by Rutherford (1911). In its original form the Rutherford formula treated only the angular distribution of the scattered particle but it can be recast in terms of the momentum transfer and converted to a SDCS as a function of the energy transfer Q. For a projectile of speed v making a collision with a free electron of mass m_e, this modified cross section is

$$\sigma_R(Q) = \frac{4\pi a_0^2 Z_1^2 R^2}{TQ^2}. \qquad (2.3)$$

where a_0 is the Bohr radius, R the Rydberg energy, and T the (nonrelativistic) kinetic energy of an electron with the same speed v as that of the incident particle, *i.e.*,

$$T = m_e v^2/2 = E/\lambda, \qquad (2.4)$$

where λ is the mass ratio m_p/m_e and E is the projectile energy.

Although the original Rutherford equation was derived under the assumption that the target is free and at rest, we may use Eq. 2.3 as an approximate cross section for ejecting a bound electron with kinetic energy ϵ, where ϵ and Q are related by Eq. 2.2. The modified Rutherford cross section should provide reasonable predictions for the production of secondary electrons when $\epsilon \gg B$ except that for ion impact there is the additional restriction that $\epsilon < 4T$ (see Section 4.4.1).

Because of its simplicity in predicting the production of energetic secondary electrons, Eq. 2.3 has been used extensively in modeling the behavior of fast charged particles passing through matter. One should, however, note the limitations of the modified Rutherford cross section (to be referred to as the Rutherford cross section hereafter for brevity):

(a) The conversion of momentum transfer into energy transfer is a poor approximation if much of the energy transfer is used to overcome the binding energy, *i.e.*, when

$$\epsilon < B. \qquad (2.5)$$

Hence, the Rutherford cross section is unreliable for describing the production of slow secondary electrons.

(b) While the original Rutherford equation is quantum mechanically (and classically) correct for the scattering of two free charged particles, it is not a rigorous solution for a bound target particle. As will be explained shortly, contributions from the dipole interaction dominate the production of secondary electrons from an atom by a fast charged particle. The Rutherford cross section does not account for any dipole interaction either in its original or modified form. Hence, the Rutherford cross section should not be used to describe collisions of fast charged projectiles (T > 10B) producing slow secondary electrons (ϵ < 100 eV) unless extra terms are introduced to account for the ionization by the dipole interaction. On the other hand, the Rutherford cross section is a good approximation for the ejection of fast secondary electrons by slow heavy projectiles when the dipole interaction is unimportant. This is one of the reasons that semiclassical theories work well for slow, heavy projectiles.

2.4 Mott Cross Section

A refinement to the Rutherford cross section is the introduction of the electron-exchange effect in the case of electron-impact ionization. Mott (1930) generalized the Rutherford cross section to account for the indistinguishability of the scattered and ejected electrons. The cross section for the collision of a free electron with another at rest (Landau and Lifshitz, 1960) may be modified, as for the Rutherford equation, to apply to a bound electron (Kim, 1975) resulting in the equation:

$$\sigma(\epsilon) = \frac{4\pi a_0^2 R^2}{T}\left[\frac{1}{Q^2} - \frac{1}{Q(T-\epsilon)} + \frac{1}{(T-\epsilon)^2}\right], \quad (2.6)$$

where $Q > 0$, $\epsilon_{max} = T - B$ for a bound electron, and hence $T - \epsilon > 0$.

The first term in the square brackets of Eq. 2.6 is the familiar Rutherford cross section, or the direct term, while the second term represents the interference between the direct and exchange terms, and the last term represents the pure exchange interaction. The quantity $T - \epsilon$ represents the energy of the scattered electron after ionization and hence could have been changed to $T - Q$. It was, however, left unchanged in order (a) to keep Eq. 2.6 from diverging at the maximum energy transfer, $Q = T$, and (b) to make the equation symmetric for the scattered (primary) and ejected (secondary) electrons.

Since Eq. 2.6 is symmetric, we now adhere to the definitions of primary and secondary electrons, *i.e.*, the slower of the two electrons emerging after an ionizing collision is labelled as the secondary electron. Hence, its maximum kinetic energy is one-half of the available energy,

$$\epsilon_{max}(\text{secondary}) = (T - B)/2. \quad (2.7)$$

Double counting will result if an integration over ϵ is extended beyond ϵ_{max}(secondary) given by Eq. 2.7.

2.5 Binary Encounter Approximation (BEA)

To account for electron binding, the Rutherford theory may be modified to include the momentum distribution of the bound electron. The term "binary encounter approximation" (BEA) is used as a generic name for theories in which some kind of momentum distribution is associated with each target particle. A common practice in a semiclassical collision theory is to derive the momentum distribution from a wave function for the target electron, while treating the motion of the projectile classically.

2.5.1 BEA Without Exchange

A simple form of the binary encounter approximation, (Williams, 1927; Inokuti, 1971; Bichsel, 1993), modifies the Rutherford cross section by using the average kinetic energy U defined by

$$U \equiv \langle p^2 \rangle/(2m_e), \quad (2.8)$$

where $\boldsymbol{p}$ is the momentum operator of each bound electron:

$$\sigma(Q) = \sigma_R\left(1 + \frac{4U}{3Q}\right). \quad (2.9)$$

Equation 2.9 is the BEA cross section for one bound electron.

For a many-electron target, one must use the appropriate B and U for each subshell, multiply the subshell cross sections by the corresponding occupation numbers and then sum over all subshells in the target. Unfortunately, experimental SDCSs available in the literature are functions of ϵ but not Q for each subshell, so

$$\sigma(\epsilon) = \frac{4\pi a_0^2 Z_1^2 R^2}{T}\sum_j N_j\left[\frac{1}{Q_j^2} + \frac{4U_j}{3Q_j^3}\right], \quad (2.10)$$

where the summation is over subshells, N_j and U_j are the occupation number and the average kinetic energy of the jth subshell, respectively, with

$$Q_j = \epsilon + B_j, \quad (2.11)$$

B_j being the corresponding subshell binding energy. Average kinetic energies, occupation numbers and binding energies are listed for some atoms and molecules in Table 2.1.

Because of kinematic restrictions, this equation requires modification for use with ion impact. Thomas (1927) first gave the correct formulation which will be discussed in Section 4.4.

TABLE 2.1—*Binding* (B) *and kinetic* (U) *energies (eV) and occupation numbers* (N) *of rare gases and simple molecules.*[a]

	He			Ne			Ar			Kr			Xe		
Orbital	*B*	*U*	*N*	*B*	*U*	*N*	*B*	*U*	*N*	*B*	*U*	*N*	*B*	*U*	*N*
1s	24.59	39.51	2	866.9	1259.1	2	3202.9	4192.9	2	14325.6	17146.1	2	34561.4	38899.6	2
2s				48.47	141.88	2	326.0	683.1	2	1921.0	3406.9	2	5452.8	9240.0	2
2p				21.60	116.02	6	249.18	651.4	6	1692.3	3375.0	6	4889.4	8229.7	6
3s							29.24	103.5	2	295.2	829.8	2	1093.2	2481.8	2
3p							15.82	78.07	6	216.8	773.7	6	957.7	2412.9	6
3d										93.0	650.3	10	672.3	2283.8	10
4s										27.5	115.8	2	213.8	696.9	2
4p										14.22	82.72	6	146.7	635.3	6
4d													68.21	495.7	10
5s													23.3	110.4	2
5p													12.56	79.74	6

	H_2			N_2			O_2				H_2O		
Orbital	*B*	*U*	*N*	*B*	*U*	*N*	*B*	*U*	*N*	Orbital	*B*	*U*	*N*
$1\sigma_g$	15.43	15.98	2	409.9	601.78	2	543.5	794.84	2	$1a_1$	539.7	1589.5	2
$1\sigma_u$				409.9	602.68	2	543.5	795.06	2	$2a_1$	36.88	70.71	2
$2\sigma_g$				41.72	71.13	2	46.19	79.73	2	$1b_1$	19.83	48.36	2
$2\sigma_u$				21.00	63.18	2	29.82	90.92	2	$3a_1$	15.57	59.52	2
$1\pi_u$				17.07	44.30	4	19.64	59.89	4	$1b_2$	12.61	61.91	2
$3\sigma_g$				15.58	54.91	2	19.79	71.84	2				
$1\pi_g$							12.07	84.88	2				

[a] Data on rare gases from Rudd *et al.* (1992). Data on molecules from Hwang *et al.* (1995).

2.5.2 BEA With Exchange (BEAX)

For incident electrons, one can follow the example of the Mott cross section and modify the BEA cross section, Eq. 2.9, so that the resulting expression is symmetric with respect to the primary and secondary electrons. One such cross section, to be referred to as the BEA with exchange, or BEAX for short, was given by Vriens (1969). For a single bound electron it is

$$\sigma(\epsilon) = \frac{4\pi a_0^2 R^2 Z_1^2}{T+U+B} \times \left\{ \frac{1}{Q^2} - \frac{1}{Q(T-\epsilon)} + \frac{1}{(T-\epsilon)^2} + \frac{4U}{3}\left[\frac{1}{Q^3} + \frac{1}{(T-\epsilon)^3}\right]\right\}. \quad (2.12)$$

The term in the square brackets of Eq. 2.12 is an approximation to introduce electron exchange. A rigorous theory would have introduced all possible combinations of Q and $T-\epsilon$ in the denominator with a total power of three, as is the case in the Mott cross section, which contains all combinations with powers of two. For a multishell target, Eq. 2.12 should be summed over subshells.

2.6 Born Approximation

Reliable theoretical methods exist to treat fast collisions, *viz.*, those collisions in which the projectile speed far exceeds (by a factor of 10 or more) the orbital speeds of bound target electrons. Many of these methods are variants of the first Born approximation (Bethe, 1930). In this approximation, the interaction between the projectile and a bound electron is treated in the first order perturbation, while the projectile and bound electrons in a target atom or molecule are separately described using appropriate wave functions. For instance, in the plane-wave Born approximation (PWBA), the projectile before and after a collision is described by plane waves, while the initial and final states of the target atom may be described by Hartree-Fock or even better wave functions as needed. If the target is an ion, Coulomb waves are used for the projectile, leading to the Coulomb-Born approximation. One can go one step further and use numerical continuum wave functions for the projectile, where these wave functions are the solutions of the Schrödinger equation (or the Dirac equation if the incident electron is very fast, say 100 keV or higher, or the target is a heavy atom or a tightly bound electron is ionized) with an effective potential representing the charge distribution of bound electrons in the target atom. This is called the distorted-wave Born approximation (DWBA).

Although both plane and Coulomb waves of a given energy can be expressed in terms of analytic functions independent of angular momentum, only plane waves allow us to express collision matrix elements in a general form independent of angular momentum (the CDW-EIS method, discussed in Section 2.11, is an exception). For the Coulomb and distorted waves we must resort to an infinite expansion of each continuum wave function in terms of angular momentum (known as the partial-wave expansion), thus

requiring double summations over the angular momenta of the incident and scattered waves. In addition, if a Coulomb or distorted wave is used for the ejected electron, then it also must be expanded in partial waves, leading to a collision cross section that involves triple summations. The number of partial waves needed increases rapidly as the projectile or ejected electron energy increases, eventually making it impractical to calculate cross sections by methods that require partial wave expansions, even with the most powerful computers presently available. The simplicity and tractability of the PWBA makes it an effective theoretical method for a wide range of radiological applications.

2.7 Plane-Wave Born Approximation (PWBA)

If the Coulomb interaction H_{int} between a projectile and a target atom (nucleus plus bound electrons) is treated in the first order perturbation, then the unperturbed Hamiltonian H_0 contains only the terms describing the nucleus and its bound electrons and the kinetic energy of the projectile:

$$H_0 = \frac{p_0^2}{2M_1} + \sum_j \left[\frac{p_j^2}{2m_e} - \frac{Z_2 e^2}{r_j} + \sum_{j>k} \frac{e^2}{r_{jk}}\right], \quad (2.13)$$

$$H_{\text{int}} = \frac{Z_1 Z_2 e^2}{r_0} - \sum_j \frac{Z_1 e^2}{r_{0j}}, \quad (2.14)$$

where the subscript 0 refers to the projectile, j and k refer to the bound electrons in the target, r_j is the distance from the target nucleus to the jth electron, and r_{jk} is the distance between the jth and kth electrons. The summations in Eqs. 2.13 and 2.14 apply to the target electrons only.

The correct solution of the wave equation involving H_0 is the product of the projectile wave function $\Phi(r_0)$ and the target wave function $\Psi(r_1,r_2,\ldots,r_N)$, since there are no operators in H_0 referring to both the projectile and the target. Letting i and f refer to the initial and final states, respectively, of the projectile and the target atom, the interaction matrix element, T_{if}, involves only the last term in Eq. 2.14:

$$T_{\text{if}} = -\langle \Phi_i \Psi_i | \sum_j Z_1 e^2 / r_{0j} | \Phi_f \Psi_f \rangle, \quad (2.15)$$

because

$$\langle \Phi_i \Psi_i | r_0^{-1} | \Phi_f \Psi_f \rangle = \langle \Phi_i | r_0^{-1} | \Phi_f \rangle \langle \Psi_i | \Psi_f \rangle \equiv 0 \quad (2.16)$$

from the orthogonality of the initial and final state wave functions in an inelastic scattering.

When plane waves are used for the projectile wave functions,

$$\Phi_i = \exp(i\mathbf{k}_i \cdot \mathbf{r}_0), \quad \Phi_f = \exp(i\mathbf{k}_f \cdot \mathbf{r}_0), \quad (2.17)$$

where $k_i\hbar$ and $k_f\hbar$ are the initial and final momenta of the projectile, respectively. Then Eq. 2.15 is simplified and becomes

$$T_{\text{if}} = 4\pi Z_1 e^2 K^{-2} \langle \Psi_i | \sum_j \exp(iK \cdot r_j) | \Psi_f \rangle. \quad (2.18)$$

The square of the matrix element T_{if} is used in the expression for the Born cross section, which is the origin of the Z_1^2 scaling of the Born cross sections.

Application of Fermi's golden rule with the interaction matrix element, Eq. 2.18, results in the familiar expression for the cross section for the ionization of an atom in the PWBA:

$$\frac{d\sigma_{\text{if}}}{d(Ka_0)^2} = \frac{4\pi a_0^2 Z_1^2 R}{T} \frac{R}{Q_{\text{if}}} \frac{df_{\text{if}}(K)/dQ}{(Ka_0)^2}, \quad (2.19)$$

where

$$Q_{\text{if}} \equiv |E_i - E_f| > 0 \quad (2.20)$$

is the energy transferred to the target, E_i and E_f are the initial and final energies of the particle, and $df_{\text{if}}(K)/dQ_{\text{if}}$ is the generalized oscillator strength (GOS),

$$df_{\text{if}}(K)/dQ = (Q_{\text{if}}/R)(Ka_0)^{-2} |\langle \Psi_i | \times \sum_j \exp(iK \cdot r_j) | \Psi_f \rangle|^2. \quad (2.21)$$

Note that, in the limit $K \to 0$, the GOS reduces to the familiar continuum dipole oscillator strength, $df_{\text{if}}(Q)/dQ$:

$$df_{\text{if}}(Q)/dQ = (Q/R) |\Psi_i| \sum_j r_j/a_0 | \Psi_f \rangle|^2, \quad (2.22)$$

again because of the orthogonality of the atomic wave functions. Also, note that the most important function in the Born cross section, Eq. 2.19, is the GOS, which is a function of K but not of T. Once the GOS is calculated for a given transition for all values of K, one can get angular distributions for arbitrary incident energies without recalculating the scattering matrix element. This simplification holds only for the PWBA. Eq. 2.19 in principle produces a triply differential cross section, from which the DDCS can be derived by integrating appropriate variables in the matrix element.

Although using plane waves for the projectile is a valid approximation when the projectile is fast, a plane wave is a poor approximation for an ejected electron unless it is also fast. As will be shown later, the majority of ejected electrons are slow ($\epsilon \approx B_1$ or less, where B_1 is the first ionization potential) and $\sigma(\epsilon)$ for slow ejected electrons strongly depends not only on the collision theory but also on the accuracy of wave functions used. For slow secondary electrons, one can use either a Coulomb function or a distorted-wave continuum function, though such a choice will require partial-wave expansions and more computational effort. The PWBA can be used for both electrons and heavy projectiles. In most applications, exchange terms are not introduced in the PWBA

formulas even for incident electrons because exchange terms are insignificant at high T where the PWBA is valid.

2.8 Bethe Approximation

To obtain an integrated cross section, Eq. 2.19 is integrated over the momentum transfer, which is equivalent to integrating over the scattering angle of the projectile, and also over the energy loss. The upper and lower limits of the integration are functions of the projectile mass M_1, Q and T. By dividing the integration into low and high K regions and using the fact that the GOS becomes the dipole oscillator strength in the limit $K \rightarrow 0$, Bethe succeeded in deriving an expression for the integrated cross section, $\sigma_i(T)$, (still within the first Born approximation or FBA) that clearly identified the leading energy dependence of the cross section, known as the Bethe approximation (Bethe, 1930):

$$\begin{aligned}\sigma_i(T) &= \int\int [d^2\sigma_{if}(K)/d(Ka_0)^2 dQ]\, d(Ka_0)^2\, dQ \\ &= (4\pi a_0^2 Z_1^2 R/T)[a_i \ln (T/R) \\ &\quad + b_i + c_i(R/T) + \cdots], \end{aligned} \tag{2.23}$$

where the Bethe constants a_i, b_i, c_i,. . . depend only on the properties of the target and can in principle be calculated from the GOS.

The first coefficient, also denoted M_1^2 (Miller and Platzman, 1954), is closely related to the integral of the continuum dipole oscillator strength:

$$a_i = \int (R/Q)[df(Q)/dQ]\, dQ, \tag{2.24}$$

but other coefficients are more complicated (Kim and Inokuti, 1971). The Bethe approximation also holds for the singly differential cross section in which the Bethe constants are now functions of Q but not T, and the integration over Q in Eq. 2.24 is omitted for a_i.

If dependable experimental photoionization cross sections are available, one can then determine the a_i coefficient from such data. For dipole-forbidden transitions, $a_i = 0$ because $df(Q)/dQ = 0$. Note that the Bethe cross section diminishes as $T^{-1}\ln T$ as T increases for a dipole-allowed transition but diminishes much faster ($\propto T^{-1}$) for a forbidden transition. Cross sections for spin-changing collisions vanish in the FBA as formulated here.

The Bethe cross section is an asymptotic form, *i.e.*, for high incident energies. This compact form applies to all types of inelastic scattering cross sections, as long as the cross section is integrated over the scattering angle of the projectile after a collision. However, terms left out in the PWBA, such as the distortion of the projectile wave function near the target and exchange terms if the projectile is an electron, enter into the asymptotic expansion, Eq. 2.23, between the second and third terms. In other words, the first two terms, those associated with a_i and b_i, in the Bethe approximation represent the essence of the PWBA. We expect, therefore, that comparisons of experiments with the PWBA will be meaningful only at high T where the Bethe approximation and the full PWBA result agree well numerically.

In Table 2.2 we list the Bethe constants for ionization, a_i, b_i and c_i of H and He as well as some of their isoelectronic ions. The constant c_i depends on the projectile mass. We caution the reader again that other T-dependent corrections must be added to the Bethe cross section for it to become reliable at T lower than about 10 times the threshold energy. Nevertheless, the Bethe formula agrees better with experimental data at low T for heavy projectiles than for electron impact.

2.9 Platzman Plot

A simple but very powerful way to graphically represent singly differential cross sections was used by Miller and Platzman (Miller, 1956). In this method, which we shall refer to as the Platzman plot, the ratio Y of $\sigma(\epsilon)$ to the Rutherford cross section for a single target electron, Eq. 2.3, is plotted as a function of R/Q:

$$Y = \sigma(\epsilon) TQ^2/4\pi a_0^2 Z_1^2 R^2, \tag{2.25}$$

where $\sigma(\epsilon)$ can be either an experimental or a theoretical SDCS. If the target is a multishell atom, $Q_1 = \epsilon + B_1$, where B_1 is the lowest binding energy, is used instead of Q in Eq. 2.25. Then

$$\begin{aligned}\int Y\, d(R/Q) &= \frac{T}{4\pi a_0^2 Z_1^2 R} \int \sigma(\epsilon)\, d\epsilon \\ &\equiv const. \times \sigma_i, \end{aligned} \tag{2.26}$$

where σ_i is the total ionization cross section. This shows that the area under a Platzman plot is proportional to the total ionization cross section. This fact can be used to normalize $\sigma(\epsilon)$ because σ_i is often known with a better accuracy than $\sigma(\epsilon)$ from independent measurements.

The quantity Y can be interpreted as the effective number of target electrons participating in an ioniz-

TABLE 2.2—*Bethe constants in Eq. (2.23) for ionization of H, He^+, H^-, He and Li^+* [a]

	a_i	b_i	$c_i(e^-)$[b]	$c_i(p)$[c]
H	0.2834	1.2566	−2.6294	−0.6619
He^+	0.07085	0.2159	−2.6294	−0.6619
H^-	7.484	25.11	−5.545	−1.045
He	0.489	0.714	−5.519	−1.209
Li^+	0.1445	0.137	−5.439	−1.276

[a] After Kim and Inokuti (1971).
[b] $c_i(e^-)$ for electron-impact ionization.
[c] $c_i(p)$ for ionization by proton and heavy ions.

ing collision. In this way, we expect that the value of Y will approach the number of valence electrons as ϵ becomes very large compared to the valence shell binding energy B_1, provided that the valence shell contributions dominate the ionization cross section as is the case in most atoms and molecules. For slow secondary electrons, the shape of the Platzman plot is expected to follow that of the continuum dipole oscillator strength (multiplied by the energy transfer, see Eqs. 2.25 and 2.26) scaled by some function of ϵ and T and superposed on the contributions from close collisions, or the Rutherford cross section. However, this scaling of the dipole contribution will be different from one atom to another. Because of the complexity of this scaling, one cannot simply add the dipole contribution to the Rutherford cross section to "synthesize" a SDCS. Nevertheless, the Platzman plot provides many useful clues to the reliability of experimental as well as theoretical SDCSs, particularly when reliable values of continuum oscillator strengths are known.

We present an example of the Platzman plot for the ionization of the Ne atom in Figure 2.1. The electron-impact experimental data of Opal *et al.* (1972) in Figure 2.1(a) may be compared with the corresponding continuum oscillator strength data in Figure 2.1(b), which were obtained from the photoionization cross sections compiled by Berkowitz (1979). The similarity in the shapes of the two curves indicates that dipole contributions are prominent at the 500 eV incident energy. Also discernible in the two sets of data near $R/Q = 0.3$, or $\epsilon = 20$ eV is a series of window resonances resulting from the interference of the 2s → np transitions with the 2p → ϵl continuum background, where l, the angular momentum of the ejected electron, can have values 0 or 2. The small dip in the electron-impact data near $\epsilon = 200$ eV is the manifestation of the interference term in the Mott cross section (Eq. 2.6), shown in the curve marked "M."

To match the known total ionization cross section, however, the data by Opal *et al.* (1972) must be renormalized to the height shown by the chained curve marked "e^-" in Figure 2.1(a). The area under the "e^-" curve reproduces the TICS measured by Rapp and Englander-Golden (1965), $\sigma_i(e^-) = 0.667\ \pi a_0^2$. The curve marked "p" is a simple extension of the e^- curve to meet the Rutherford cross section at the maximum energy that can be transferred by an incident proton with the same speed as a 500-eV electron, *i.e.*, with a kinetic energy of 0.92 MeV. The "proton-impact" curve constructed in this way and the corresponding cross section obtained from the area under the "p" curve leads to $\sigma_i(p) = 0.74\ \pi a_0^2$, in good agreement with the proton-impact experimental value of $0.72\ \pi a_0^2$ measured by Hooper *et al.* (1962).

Note that it is simple to extrapolate the electron-impact data for slow secondary electrons, $\epsilon < 5$ eV, by following the shape of the dipole contribution in Figure 2.1(b). This possibility is very important because most experimental data on secondary electrons are either unavailable or unreliable at $\epsilon < 5$ eV. The value of $\sigma(\epsilon)$ at $\epsilon = 0$ can be either measured (Grissom *et al.*, 1972) or extrapolated from the discrete excitation cross sections using the quantum defect theory (Kim and Inokuti, 1973). These threshold values are also given in Figure 2.1(a). They clearly indicate that

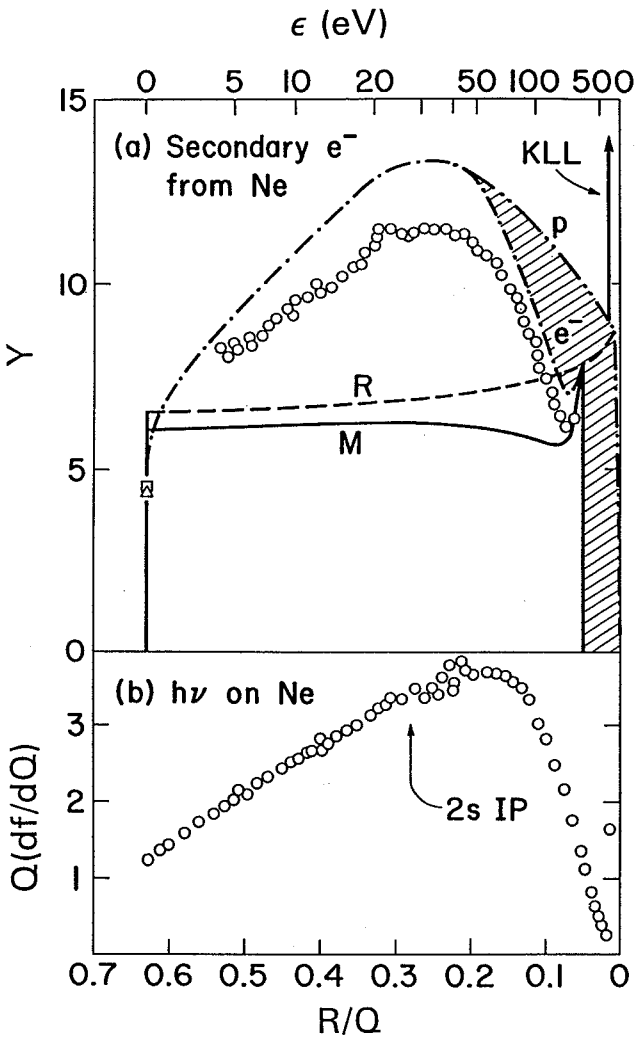

Fig. 2.1. Platzman plot of electron-impact ionization of Ne. Here, $Q = \epsilon + B_1$. (a) Circles, data of Opal *et al.* (1972) with 500-eV incident electrons; square, electron-impact experimental data by Grissom *et al.* (1972); triangle, theoretical data by Kim (based on unpublished quantum defect theory); solid curve marked "M," Mott cross section, Eq. 2.6; dashed curve marked "R," Rutherford cross section, Eq. 2.3 summed over subshells; dot-dashed curve marked "e^-," extension of the extrapolation of the experimental data (Opal *et al.*, 1972) to make the area under the curve consistent with the known TICS, which is proportional to the area under the curve; dot-dashed curve marked "p," the corresponding proton-impact cross section; shaded area, the difference between the TICS for electron and proton impact at T=500 eV (E=0.92 MeV). The vertical arrow marked "KLL" indicates the expected position of KLL Auger peaks. (b) Circles, experimental photoionization cross sections compiled by Berkowitz (1979). The arrow marked "2s IP" indicates the threshold for ionizing a 2s electron.

both the Rutherford and Mott cross sections overestimate hard-collision contributions at the threshold, although a simple extrapolation of the Rutherford or Mott cross section to $\epsilon = 0$ would have affected only the values of $\sigma(\epsilon)$ very close to the threshold.

These illustrations clearly demonstrate the power of the Platzman plot in (a) verifying the reliability of experimental cross sections, (b) normalizing the overall magnitude, and (c) extrapolating $\sigma(\epsilon)$ to values of ϵ inaccessible to experiments, as long as T is high enough so that the dipole contribution is substantial. The Platzman plot is an important tool in modeling studies of energy deposition by fast particles in which $\sigma(\epsilon)$ as a function of ϵ and T is needed.

2.10 Total Cross Section for Ionization by Ions

Discussions of the Born approximation, the Bethe theory, and the Platzman plot in Section 2.9 are applicable to ionization by bare ions such as protons and α-particles. The Bethe theory predicts that electron-impact and ion-impact cross sections will become the same if the projectile velocity is very high and the cross section is expressed in terms of the scaled T defined in terms of the projectile velocity v instead of the projectile energy E itself (Eq. 2.4).

Since the Bethe theory that predicts this similarity of cross sections does not account for the electron exchange interaction, this asymptotic behavior is achieved only at high enough T that contributions from the exchange interaction in electron-impact ionization are negligible, *i.e.*, for $T \sim 1$ keV and above.

Although an incident ion carries a considerably larger kinetic energy than an electron, the maximum amount of energy that can be transferred to a free target electron at rest is limited to $4T$ from the conservation of energy and momentum. This is known as the "classical cutoff" of energy transfer (Rudd *et al.*, 1992), and its value is considerably less than E as can be seen from Eq. 2.4.

For slow projectile ions, ionization by electron capture to the continuum (called ECC and discussed in Section 4.2.1) is significant, and theories based on the Born approximation are not applicable. The Binary Encounter Dipole (BED) model to be described in Section 3.6.2 for electron-impact ionization can be adapted to ionization by fast protons and other bare ions by omitting the electron-exchange related terms and excluding inner shells whose binding energies exceed $4T$. However, to achieve the level of success that we have seen in electron-impact ionization, the BED model must also account for ionization by the ECC mechanism, which may contribute a discernible fraction to the total ionization cross sections when T is comparable to the average kinetic energies U of target electrons in valence shells.

Since ECC involves the formation of a transient molecule consisting of the projectile and the target, the outcome depends heavily on both the internal structure of the target and the projectile speed. No simple model such as the BED model can describe such collisions.

When the incident ion also has its own bound electrons, the difficulty in describing such collisions even in qualitative terms increases rapidly with the number of electrons bound to the projectile. When the projectile is fast, we can still construct a theory based on the Born approximation. The resulting ionization cross section consists of three parts (Gillespie *et al.*, 1978): (a) the interaction of the projectile nucleus with the electrons bound to the target; (b) the interaction of the target nucleus with the electrons bound to the projectile; and (c) the interaction between electrons bound to the projectile and those bound to the target. Since the Born approximation is meaningful when the projectile T far exceeds the U's of all active electrons, the asymptotic behavior predicted by the Born approximation can be realized only when E is very high even for light ions and atoms.

2.11 Continuum-Distorted-Wave Eikonal-Initial State (CDW-EIS) Method

In the case of electron-impact ionization, it is customary to assume that the target atom or molecule is infinitely heavy compared to the incident and ejected electrons so that the center of mass of the colliding system does not move before and after the collision. In the case of ion-impact ionization of light atoms or molecules, the center of mass moves along the line between the target nucleus and the projectile ion. Hence, even for the plane-wave Born approximation, it is necessary to include the motion of the center of mass in the plane waves for the ion projectile. The ejected electron is represented by a plane or Coulomb wave centered on the residual ion, but does not refer to the scattered ion. The interaction between the projectile and the target electron (before and after the collision) is treated in first order perturbation.

However, a more accurate description at a large distance from the target before the collision should include the distortion of the (bound) target electron wave function due to the attraction of the projectile ion, and similarly the description of the target after the collision should include the distortion of the ejected electron wave function due to the attraction of both the residual ion and the scattered ion, even though one may still describe the motion of the projectile ion as a plane wave (*i.e.*, having a straight line trajectory) including the moving center of mass. In other words, the PWBA does not satisfy the asymptotic conditions both before and after the collision.

The CDW-EIS method (Fainstein *et al.*, 1991b) compensates for this deficiency by adding more phase factors to the PWBA initial- and final-state wave functions. These phase factors partly account for the interaction of the target electron with the projectile before and after the collision. The interaction unaccounted for in this way is then treated in first-order perturbation. The CDW-EIS method has been successfully applied to target atoms with simple shell structures, *e.g.*, H and He, ionized by bare ions. In all cases, the CDW-EIS method agrees better than the PWBA with experimental values of DDCSs and SDCSs. The ejected-electron wave function is usually expressed in terms of Coulomb functions with an effective nuclear charge, which allows one to obtain analytic expressions for the interaction matrix elements. Unlike the PWBA, two-center effects are built into the wave functions in the CDW-EIS method, and hence the latter describes both direct ionization and ionization due to electron capture to the continuum states of the projectile. Many examples are illustrated in a comprehensive review by Fainstein *et al.* (1991).

Although the application of the CDW-EIS method to proton-neon collisions (Fainstein *et al.*, 1991a) indicates that the method reproduces all of the major features of DDCS, the use of simple Coulomb functions for the ejected electron is likely to introduce uncertainties in the cross section for ejecting slow electrons, which dominate the SDCS and TICS. In view of its outstanding success in describing various features of the two-center effects, this method deserves more systematic studies with radiological applications in mind.

2.12 Classical-Trajectory Monte Carlo (CTMC) Method

In this method (Abrines and Percival, 1966; Olson and Salop, 1977), the coupled classical Hamiltonian equations of motion are solved. These equations govern the motion of three particles—the incident ion, the target nucleus, and the electron being ionized∫nteracting with each other through Coulomb potentials. Since classical mechanics is used, the motion of each particle in the three-dimensional space is described by three components of the momentum vector and three components of the position vector, thus making it necessary to solve a total of 18 coupled equations. Initial conditions of the incident ion and the orbital motion of the electron around the nucleus are sampled appropriately and then large numbers (10^4 to 10^7) of trajectories of the ion are calculated by solving the coupled equations numerically. Since the errors in the resulting cross sections depend on the number of trajectories used, the CTMC method is computationally expensive for collision processes with very small cross sections. However, the method is effective for calculating differential cross sections for direct ionization as well as for electron capture to bound and continuum states of the projectile ion.

The CTMC method has had considerable success in describing ionization of simple atoms by bare ions of moderate incident energies, up to a few hundred keV/u. However, the CTMC method has one built-in difficulty: pure classical theory—basically equivalent to the Rutherford equation discussed in Section 2.3—lacks contributions from the dipole interaction (Olson, 1983; Reinhold and Burgdörfer, 1993), which becomes dominant for fast incident ions of energies of about 1 MeV/u and greater. As is the case for the CDW-EIS method, more systematic studies are needed to better understand the limitations of the CTMC method in radiological applications.

2.13 Consistency Requirements

Even though theory cannot always predict accurate ionization cross sections, certain aspects of theory are so well founded that they can be used to (i) identify certain limitations, (ii) provide relationships among different kinds of collision data, and (iii) supply information on the expected asymptotic behavior in certain energy regimes. These requirements help us to judge the reliability of various types of cross sections, both theoretical and experimental. There are six major requirements to be satisfied by TICSs, SDCSs, and DDCSs (Kim, 1983b).

(A) Threshold behavior

Ionization cross sections must first satisfy the trivial requirement that the cross sections vanish at the threshold. Since most measurements of DDCSs are made at incident energies well above the lowest ionization threshold of a given target, measured DDCSs should vanish when extrapolated to the threshold. For electron impact the threshold energy is equal to the binding energy, *i.e.*, $E = B$. For ion impact, the threshold is not as well defined and few, if any, measurements have been made near this threshold.

(B) Asymptotic (high T) behavior

According to the Bethe theory (Eq. 2.23), when $\sigma_i(T)T/4\pi a_0^2 Z_1^2 R$ is plotted against $\ln(T/R)$—this type of plot is known as the Fano plot—the slope of the resulting curve at high T is a_i defined by Eq. 2.24, which in turn can be deduced from photoionization cross sections. For most atoms and molecules of interest in radiation research, photoionization cross sections have been more accurately measured than electron-impact or ion-impact ionization cross sections. This requirement also holds for the SDCS and

DDCS. For the SDCS, $\sigma(\epsilon)$ and $df(Q)/dQ$ (without integration) are used to construct the Fano plot. For the DDCS, $\sigma(\epsilon,\theta)$ and $d^2f(Q,\theta)/dQd\Omega$ are used instead.

(C) Angular Symmetry in the Slope of the Fano Plot

Since the angular distribution of photoelectrons has the form $a + b\cos^2\theta$, the differential photoionization cross section is the same for two supplementary angles, *i.e.*, for θ_1 and θ_2 such that $\theta_1 + \theta_2 = 180°$. Hence, the slopes of the Fano plots of the DDCS for a given ϵ for a pair of supplementary angles should be the same (Kim, 1972). This test of forward-backward symmetry can reveal subtle systematic problems in experimental DDCSs. To use the Fano plot for this consistency test, however, cross sections at rather high T (at least $\geq$ 1 keV) must be used. Otherwise, the cross sections may not have reached asymptotic behavior and consequently may lead to erroneous conclusions.

(D) Integrated Cross Sections

Often DDCS measurements are relative, and they must be normalized to integrated cross sections such as σ_i. The integration of the DDCS over θ to obtain the SDCS is insensitive to the DDCS values at the extreme forward and backward angles because of the $\sin\theta$ in $d\Omega = 2\pi\sin\theta d\theta$. Nevertheless, comparisons with σ_i, which are usually measured independently of the DDCSs and more accurately, serve as an important indicator of the reliability of the DDCSs. It is impractical to measure DDCSs at $\epsilon = 0$, because such secondary electrons will not reach the detector, which is placed some distance from the collision volume. Hence, the values of DDCS at $\epsilon = 0$ must be deduced by extrapolating cross sections for $\epsilon > 0$. The consistency of such an extrapolated DDCS can be checked by first integrating the DDCS over θ to get the SDCS at $\epsilon = 0$. Then, the quantum-defect theory (Kim and Inokuti, 1973) connects $\sigma(\epsilon = 0)$ to the total cross section for discrete excitation σ_n at the same incident energy through the relation:

$$\lim_{n\to\infty} \frac{(n^*)^3}{2}\sigma_n = \sigma(\epsilon = 0), \qquad (2.27)$$

where n^* is the effective quantum number and σ_n is the sum of all discrete-excitation cross sections with the same principal quantum number n that corresponds to n^*. For multishell targets, the left-hand side of Eq. 2.27 must be the sum over all Rydberg series approaching the first ionization limit.

(E) Energy-Loss Cross Section and SDCS

When single ionization dominates, *i.e.*, when multiple ionization, excitation and inner-shell ionization can be ignored, cross sections for the energy loss of the projectile can be matched with the SDCS for electron ejection. However, the angular distribution of the scattered particle and the DDCS of the ejected electron cannot be compared because the former is sharply peaked in the forward direction while the latter is spread over all angles.

(F) Binary Peak Position

As was mentioned in Section 2.2, fast secondary electrons are ejected by knock-on collisions and the ejection angle θ_B of such electrons, called the binary peak, is well defined by Eq. 2.1. Binary peaks will be relatively narrow if the electron is ejected from a loosely bound orbital and broad if it is ejected from a tightly bound orbital. If a coarse angular mesh is used in the measurement of DDCS, the binary peak for some values of ϵ may fall between the measured angles and appear as a sudden drop in the SDCS when the DDCS is integrated.

2.14 Projectiles at Relativistic Speeds

For projectiles with relativistic speeds ($v/c \geq 0.1$) the nonrelativistic formulations used so far become inaccurate and different expressions must be used. First of all, the scaled incident kinetic energy T now must be expressed in terms of the quantity $\beta = v/c$:

$$T/R = (\tfrac{1}{2}m_e v^2)/(\tfrac{1}{2}m_e c^2\alpha^2) = \beta^2/\alpha^2, \qquad (2.28)$$

where $\alpha \approx 1/137$ is the fine structure constant. At relativistic speeds the Bethe theory is very reliable and the first two terms in Eq. 2.23 are sufficient to accurately describe σ_i (Bethe, 1932). Using the relativistic expressions for the limits of integration and for the Coulomb interaction, the equation becomes

$$\sigma_i(\beta^2) = \frac{4\pi a_0^2\alpha^2 Z_1^2}{\beta^2}\left\{a_i\left[\ln\left(\frac{\beta^2}{1-\beta^2}\right) - \beta^2\right] + b_i'\right\}, \qquad (2.29)$$

where a_i is the same Bethe constant used in the nonrelativistic formula, Eqs. 2.23 and 2.24, and b_i' is related to the b_i in Eq. 2.23 by the relation

$$b_i' = b_i - 2a_i \ln\alpha = b_i + 9.840a_i. \qquad (2.30)$$

For incident electrons with relativistic speeds, the Coulomb interaction must be supplemented by a relativistic correction. For the SDCS, the relativistic counterpart of the Mott cross section described in Section 2.4 is known as the Møller cross section (Bethe and Ashkin, 1953). We now denote kinetic energies of the incident electron by E and that of the ejected electron by ϵ. Note that the relativistic kinetic energy is defined as the total energy minus the rest energy, $m_e c^2$. The original Møller cross section is for the relativistic scattering of two free electrons, and hence diverges for $\epsilon = 0$ as the original Mott cross section did. To avoid this difficulty, we add the binding energy to the terms that diverge at $\epsilon = 0$ as

we did to modify the Rutherford and Mott cross sections:

$$\sigma(\epsilon) = \frac{4\pi a_0^2 \alpha^2 R}{\beta^2} \cdot \sum N_j \left[\frac{1}{(\epsilon + B_j)^2} + \frac{1}{(E - \epsilon)^2} + \frac{1}{(E + m_e c^2)^2} - \frac{1}{(\epsilon + B_j)(E - \epsilon)} \times \frac{m_e c^2 (2E + m_e c^2)}{(E + m_e c^2)^2} \right], \quad (2.31)$$

which has the dimension of area per energy unit used for ϵ, B_j and E. Eq. 2.31 is correct even when both the primary electron energy E and the secondary electron energy ϵ are relativistic. The Møller cross section, however, still lacks contributions from the dipole interaction just as the Mott cross section did. The binary peak for the ejected electron is in the direction of

$$\cos \theta_B = [Q(E + 2m_e c^2)/E(\epsilon + 2m_e c^2)]^{1/2}, \quad (2.32)$$

which reduces to Eq. 2.1 in the nonrelativistic limit.

3. Electron Interactions

3.1 Introduction

Secondary electrons ejected from atoms or molecules by any kind of radiation become primary particles in all subsequent collisions and, as mentioned previously, most radiological effects involve interactions of electrons with matter. It is therefore necessary to understand the systematics of secondary electron production in making calculations of radiation effects. Cross section functions (total ionization cross sections versus incident electron energies) must be known, as well as differential cross sections. In this section we will describe the experimental and theoretical methods for obtaining differential, partial and total electron impact ionization cross sections for atoms, molecules and clusters. Data will be presented and discussed critically.

3.2 Ionization Mechanisms and Definitions

Electrons accelerated through a potential of several tens of volts have a de Broglie wavelength of about 0.1 nm. Since this wavelength is similar to molecular dimensions, mutual distortions occur, that is, an electron may be promoted from a lower to a higher orbital or - if the electron energy is greater than a critical value (the ionization energy or appearance energy) - an electron may be ejected from the target, thus producing a positive ion.

Direct attachment of the incident electron to an atomic target to give a stable negative ion is less likely. The reason for this is that the momentum and translational energy of the attaching electron and the binding energy (electron affinity) must be absorbed by the emerging product. Usually, the excess energy leads either to fragmentation (in the case of a molecular target) or to detachment of the electron.

As the electron energy is increased, the variety and abundance of the ions produced from a specific molecular target will increase, because the electron ionization process may proceed via different reaction channels, each of which gives rise to characteristic ionized and neutral products (Märk, 1982a; 1985). These include the parent ion, fragment ion, multiply-charged ion, excited ion, metastable ion, rearrangement ion, and ion pair. For the simple case of a diatomic molecule AB these reaction channels are:

$AB + e \rightarrow$

$AB^+ + e_s + e_e$	(single ionization)	(3.1)
$AB^{2+} + e_s + 2e_e$	(double ionization)	(3.2)
$AB^{z+} + e_s + ze_e$	(multiple ionization)	(3.3)
$AB^{K+} + e_s + e_e$	(K-shell ionization)	(3.4)
$AB^{**} + e_s \rightarrow AB^+ + e_s + e_e$	(autoionization)	(3.5)
$AB^{+*} + e_s + e_e \rightarrow A^+ + B + e_s + e_e$	(fragmentation)	(3.6)
$\rightarrow AB^{2+} + e_s + 2e_e$	(autoionization)	(3.7)
$\rightarrow AB^+ + e_s + e_e + h\nu$	(radiative ionization)	(3.8)
$A^+ + B + e_s + e_e$	(dissociative ionization)	(3.9)
$A^+ + B^- + e_s$	(ion pair production)	(3.10)
$AB^* + e_s$	(excitation)	(3.11)
AB^{-*}	(attachment)	(3.12)
$A^- + B$	(dissociative attachment)	(3.13)
$A + B + e_s$	(dissociation into neutrals)	(3.14)
$A^* + B + e_s$	(dissociation into neutrals).	(3.15)

In the above e_s is the *scattered* incident electron and e_e an *ejected* secondary electron. Other products may be obtained, especially when one is using complex targets, *e.g.*, polyatomic molecules (Märk, 1984) or clusters (Märk, 1987; 1991; 1994; Märk and Castleman, 1985).

Most of the ionization reactions summarized above (*e.g.*, process 3.1 through 3.4, and 3.9) can be classified as direct ionization events, in which the ejected and the scattered electrons leave the ion within 10^{-16} s. Conversely, there exist alternative ionization channels competing with direct ionization in which the electrons are ejected one after the other. Figure 3.1 shows a schematic representation of possible ionization mechanisms (Märk, 1986). For instance, autoionization (processes 3.5 and 3.7) can be described as a two-step reaction. First, a neutral molecule or atom is raised to a superexcited state which can exist for some finite time. Then, a radiationless transition into the continuum occurs. For molecules, the autoionization rate (and hence the ionization cross section) is limited by the characteristic energy-storage mode frequency. If predissociation into two neutrals is faster than autoionization, the latter will not occur at an appreciable rate. Moreover, autoionization is a resonance process which complicates the ionization cross-section dependence at low electron energy. For example, it may cause a deviation from the threshold law (Märk, 1984). There may also be an effect at higher electron energies as in the example in Figure 3.2 showing the partial ionization cross-section function for the production of Ar^+. The top curve shows the variation of the cross-section function obtained by summing over all possible ionization mechanisms.